

# Kinetics of $\beta$ - $\text{Si}_3\text{N}_4$ Grain Growth in $\text{Si}_3\text{N}_4$ Ceramics Sintered under High Nitrogen Pressure

Kou-Rueh Lai\* and Tseng-Ying Tien\*

Materials Science and Engineering, The University of Michigan, Ann Arbor, Michigan 48109

The kinetics of anisotropic  $\beta$ - $\text{Si}_3\text{N}_4$  grain growth in silicon nitride ceramics were studied. Specimens were sintered at temperatures ranging from 1600° to 1900°C under 10 atm of nitrogen pressure for various lengths of time. The results demonstrate that the grain growth behavior of  $\beta$ - $\text{Si}_3\text{N}_4$  grains follows the empirical growth law  $D^n - D_0^n = kt$ , with the exponents equaling 3 and 5 for length [001] and width [210] directions, respectively. Activation energies for grain growth were 686 kJ/mol for length and 772 kJ/mol for width. These differences in growth rate constants and exponents for length and width directions are responsible for the anisotropy of  $\beta$ - $\text{Si}_3\text{N}_4$  growth during isothermal grain growth. The resultant aspect ratio of these elongated grains increases with sintering temperature and time.

## I. Introduction

SILICON NITRIDE ceramics have become increasingly promising materials for heat engine applications because of their excellent performance in high-temperature environments.<sup>1,2</sup> It is known that the interlocking elongated  $\beta$ - $\text{Si}_3\text{N}_4$  grains are responsible for the high fracture toughness of these materials.<sup>3</sup>

Silicon nitride ceramics with elongated  $\beta$ - $\text{Si}_3\text{N}_4$  grains have been developed by pressureless sintering,<sup>4</sup> hot-pressing,<sup>5,6</sup> hot isostatic pressing,<sup>7</sup> and gas pressure sintering.<sup>3,8-10</sup> However, previous studies on the development of silicon nitride ceramics have been limited to observation of the relations between mechanical properties and compositions of the ceramics. Only a few authors<sup>4,11-13</sup> have contributed to the understanding of the grain growth mechanisms of elongated  $\beta$ - $\text{Si}_3\text{N}_4$  grains. By considering the anisotropy of interfacial energy of facet grains such as  $\beta$ - $\text{Si}_3\text{N}_4$ , Lee *et al.*<sup>12</sup> concluded that the mechanism of  $\alpha$ - $\beta$  phase transformation, as well as the grain growth of  $\beta$ - $\text{Si}_3\text{N}_4$ , were interface-reaction-controlled, which implies that the growth exponent  $n = 2$ . However, they determined the grain size of elongated  $\beta$ - $\text{Si}_3\text{N}_4$  grains in such a way that anisotropy of elongated grains was ignored. Their results<sup>12</sup> therefore can lead to erroneous conclusions.

In contrast, Hwang<sup>4</sup> and Mitomo *et al.*<sup>11</sup> incorporated shape and size factors and considered the dimensions of length and width, which correspond to the crystal axes of [001] and [210] of  $\beta$ - $\text{Si}_3\text{N}_4$ , for the measurements of an elongated grain. The aspect ratio was defined as the ratio of length to width. In general, the aspect ratio is an indication of the anisotropy of the elongated grain. They found that the growth behaviors of the elongated  $\beta$ - $\text{Si}_3\text{N}_4$  grains followed the empirical grain growth equation with cubic exponent in both [001] and [210] directions. These results are analogous to the Ostwald ripening

model.<sup>4,11</sup> The growth mechanism was believed to be diffusion-controlled. More specifically, the previously dissolved atoms diffused through the grain boundary layer during the liquid phase sintering of  $\beta$ - $\text{Si}_3\text{N}_4$  and sequentially precipitated onto the surface of existing  $\beta$ - $\text{Si}_3\text{N}_4$  nuclei.<sup>14</sup>

Many efforts have been made to elucidate the mechanism for the development of microstructures containing interlocking elongated grains. Several models have been proposed: (1) high interfacial energy of facet grain that leads to a lateral spreading of atom layers around either two-dimensional nuclei or screw dislocations;<sup>12,15</sup> (2) surface roughness of the facet plane that results in a high precipitation rate along the long axis;<sup>4,16</sup> (3) anisotropic grain boundary energy that causes the growth exponent to increase from 2.4 to 4;<sup>17</sup> and (4) shape preservation of grains that results in a rapid growth rate on the long axis.<sup>18,19</sup> None of these models, however, can account for the fact that the grains grow isothermally along the preferential direction of  $\beta$ - $\text{Si}_3\text{N}_4$  grains, i.e., the [001] direction. This problem might be due to the difficulty of determining the grain size of anisotropic grains using micrographs of two-dimensional (polished and etched) surfaces. These micrographs may not be sufficient for determining growth exponents accurately.

A method for measuring the grain length and width of elongated grains directly was developed in the present study. Individual  $\beta$ - $\text{Si}_3\text{N}_4$  grains were taken from the surface of the bulk specimen that was overetched by dissolving the grain boundary phases. Loose grains on the surface were disintegrated using an ultrasonic vibrator, collected at the bottom of a beaker, and used for grain size measurement. This step eliminates stereologic consideration of a two-dimensional configuration due to sections of random array grains. More consistent results were therefore obtained for successful interpretation of the growth preference of  $\beta$ - $\text{Si}_3\text{N}_4$  grains during isothermal sintering.

## II. Experimental Procedure

High  $\alpha$ -content silicon nitride powders (SN-E10  $\text{Si}_3\text{N}_4$ , Ube Co., Tokyo, Japan) ( $a > 95.5\%$ , 1.57 wt% O) were attrition milled with 10 wt%  $\text{Y}_2\text{O}_3$  (99.99%  $\text{Y}_2\text{O}_3$ , Aldrich Chemical Co., Milwaukee, WI) and  $\text{Al}_2\text{O}_3$  (AKP-50  $\text{Al}_2\text{O}_3$ , Sumitomo Chemical Co., Osaka, Japan) (with a ratio of  $\text{Y}_3\text{Al}_5\text{O}_{12}$ , labeled as B10Y) in iso(propyl alcohol) using  $\sim 2$ -mm-diameter alumina ball media for 2 h. Slurries were then dried at  $\sim 85^\circ\text{C}$  on a hot plate with magnetic stirring to prevent any sedimentation of coarse particles. Approximately 2 g of the dried powder was uniaxially pressed under 14 MPa in a die 12.5 mm in diameter. The pellet was then isostatically cold-pressed under a pressure of 160 MPa. The compact was placed in a BN crucible with a cover and heated under 10 atm (980 kPa) of  $\text{N}_2$  pressure at 1600° to 1900°C in a high-pressure furnace (Centorr Associates, Suncook, NH) for various times. To assure a minimum variation of temperature (within 5°C) during sintering, a two-color pyrometer (Model ROS, Capintec Instruments, Ramsey, NJ) was used. Phases existing in the ceramics were determined by XRD.

Sintered samples were polished and etched for microstructure observation using scanning electron microscopy. Etching

C. A. Handwerker—contributing editor

Manuscript No. 196063. Received January 9, 1992; approved August 11, 1992. Supported by U.S. Department of Energy, Office of Transportation Technologies, Advanced Materials Development Program under Contract No. DE-AC05-84OR2140, administered by Dr. D. R. Johnson of Oak Ridge National Laboratory. \*Member, American Ceramic Society.

was done by immersing the specimens into molten mixed alkali hydroxides (with a composition of  $\text{LiOH}:\text{NaOH}:\text{KOH} = 1:2:2$ ) in an Mo crucible at about  $500^\circ\text{C}$  for 15 to 30 s, depending on the porosity of the specimen. A layer of approximately 0.2 mm was removed from the etched surface (about five etchings) of the sintered specimens to eliminate the edge effect. The surface was then washed and disintegrated in water with an ultrasonic vibrator. The loose grains were collected at the bottom of a beaker and were used for grain size measurement.

A typical micrograph of disintegrated grains is shown in Fig. 1. The grain sizes of these disintegrated grains are clearly revealed and can be determined without any stereological consideration. Length and width of individual grains were measured and the results were recorded. To ensure the etching did not introduce erroneous results, measurements were made on samples etched for different lengths of time. In Fig. 2, there are no significant variations of grain size among the etchings, indicating that neither etching nor the use of ultrasonic vibration had any observable effect on the grain size measurement of silicon nitride grains.

### III. Results and Discussion

All the  $\alpha\text{-Si}_3\text{N}_4$  phases were transformed into  $\beta\text{-Si}_3\text{N}_4$  after sintering for 0.5 to 5 h at temperatures ranging from  $1600^\circ$  to  $1900^\circ\text{C}$ . Grain boundary phases in this system were identified as yttrium aluminum garnet (YAG) and residual glassy phase at room temperature. The range of relative density achieved was 98.5% to 99.3% theoretical density. Figure 3 is a typical micrograph of an etched surface of polished silicon nitride ceramics.

Results of measured average grain length, width, and the resultant aspect ratio of these samples are given in Table I. At least 500 grains were measured for each datum point to obtain essential consistent results. Average grain size for each specimen was calculated arithmetically from these individual measurements.

As Fig. 2 illustrates, the aspect ratio of the  $\beta\text{-Si}_3\text{N}_4$  follows a normal distribution. The broad distribution of the aspect ratio is in contradiction with an assumption proposed in previous studies<sup>4,11,13</sup> where a constant aspect ratio was suggested. In regard



Fig. 1. Typical micrograph of the disintegrated grains of B10Y- $\text{Si}_3\text{N}_4$  ceramics. Sample was sintered at  $1800^\circ\text{C}$  under 10-atm  $\text{N}_2$  for 1 h.

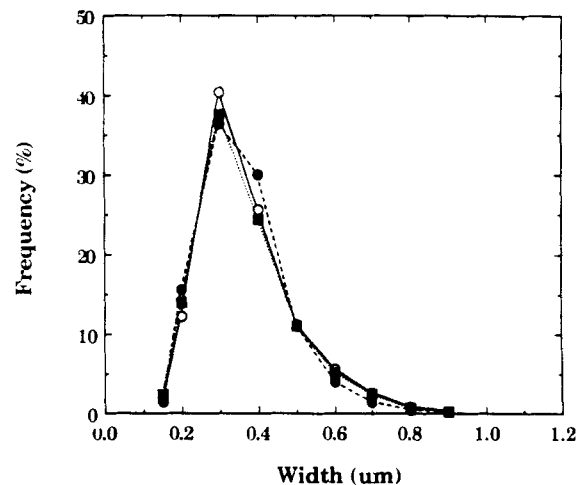
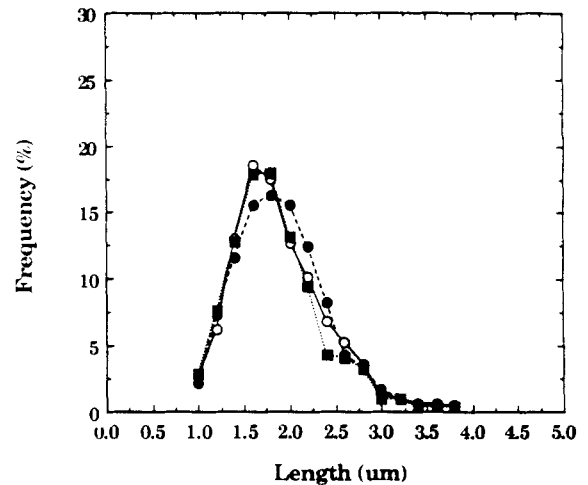
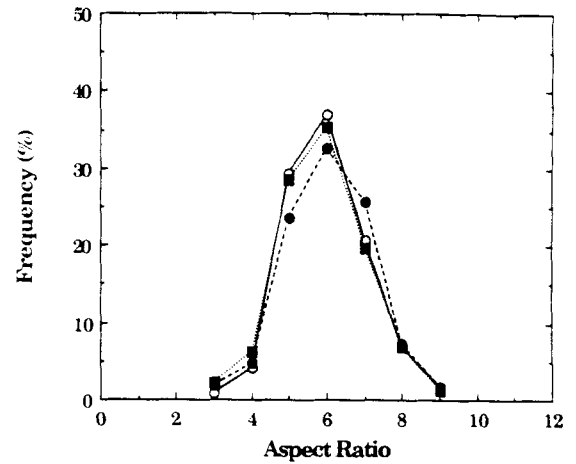


Fig. 2. Measured grain size distributions of disintegrated specimens. Sample was sintered at  $1700^\circ\text{C}$  for 1 h. —○— 30-s etching and 4-h sedimentation, —●— 120-s etching and 4-h sedimentation, —■— 120-s etching and 24-h sedimentation.

to the nature of the  $\alpha\text{-}\beta$  phase transformation of  $\text{Si}_3\text{N}_4$  ceramics, it is known that the  $\alpha\text{-}\beta$  phase transformation is a reconstructive process.<sup>14</sup> This relatively sluggish process results in a situation in which both  $\alpha\text{-}\beta$  transformation and the coarsening of  $\beta\text{-Si}_3\text{N}_4$  grains occur simultaneously. It is therefore not surprising that the aspect ratio is not a constant, but rather follows a normal distribution function.

Figure 4 presents normalized grain size ( $L/\bar{L}$  and  $W/\bar{W}$ , where  $\bar{L}$  and  $\bar{W}$  are average grain length and width, respectively) distributions of samples isothermally sintered at  $1800^\circ\text{C}$  for various times. All distributions appear to be log normal, indicating

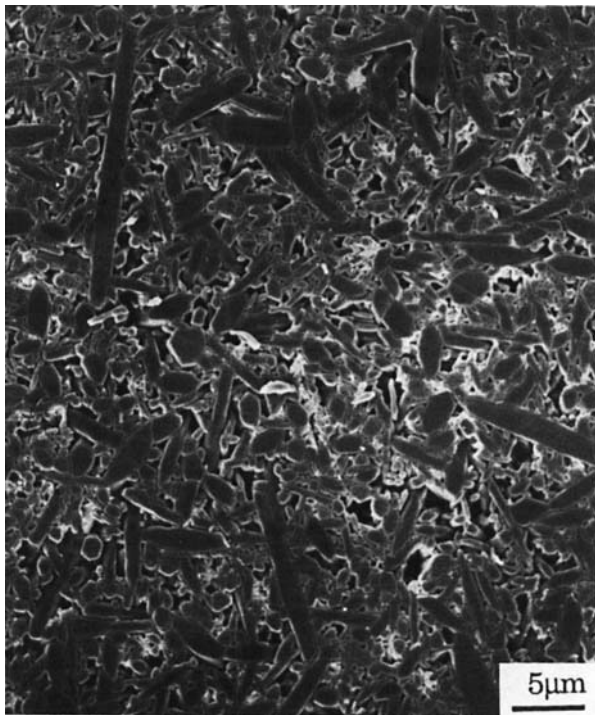


Fig. 3. Typical microstructure of B10Y-Si<sub>3</sub>N<sub>4</sub> ceramics. Sample was sintered at 1900°C under 10-atm N<sub>2</sub> for 1 h.

that normal grain growth has been reached. The broad distribution indicates that the growth mechanism reconciles with the diffusion-controlled Ostwald ripening.<sup>20</sup> As sintering time progresses, the distributions become broader and flatter. These broadened and flattened distributions might be due to the anisotropic grain boundary energies that were proposed by Grest, Srolovitz and Anderson.<sup>17</sup>

The grain growth of the anisotropic  $\beta$ -Si<sub>3</sub>N<sub>4</sub> grains is expressed by the empirical equation<sup>4</sup>

$$L^n - L_0^n = K_L t \tag{1}$$

$$W^{n_2} - W_0^{n_2} = K_W t \tag{2}$$

Table I. Measured Average Grain Sizes and Aspect Ratios of  $\beta$ -Si<sub>3</sub>N<sub>4</sub> Ceramics Sintered under 10-atm N<sub>2</sub>

Grain size ( $\mu\text{m}$ )	Sintering time (h)			
	0.5	1	2	5
1900°C-L	5.860	7.610	9.440	12.130
1800°C-L	2.910	3.890	4.860	5.790
1700°C-L	1.392	1.855	2.313	2.987
1600°C-L	0.794	0.848	1.210	1.590
1900°C-W	0.740	0.848	0.955	1.120
1800°C-W	0.441	0.523	0.565	0.657
1700°C-W	0.281	0.320	0.369	0.419
1600°C-W	0.186	0.211	2.252	0.284
1900°C-A	7.920	8.960	9.880	10.830
1800°C-A	6.590	7.430	8.300	9.090
1700°C-A	4.950	5.790	6.270	7.120
1600°C-A	4.260	4.810	4.830	5.690

where  $L$  and  $W$  are grain length and width after time  $t$ , and  $L_0$  and  $W_0$  are the initial grain length and width, which can be neglected if a high  $\alpha$ -Si<sub>3</sub>N<sub>4</sub> starting powder is used.  $K_L$  and  $K_W$  are rate constants in the length and width directions, respectively. The aspect ratio (AR) can be further written as

$$AR = \frac{L}{W} = \frac{(K_L)^{1/n_1}}{(K_W)^{1/n_2}} t^{[(1/n_1) - (1/n_2)]} \tag{3}$$

The rate constant of the growth equation<sup>21,22</sup> can be expressed as

$$K = \frac{8D\gamma V_m C_\alpha}{9RT} \tag{4}$$

where  $D$  is the volume diffusivity of the diffusing species,  $\gamma$  is the specific surface free energy of the particle/matrix interface,  $V_m$  is the molar volume of the precipitate,  $C_\alpha$  is the equilibrium solute content in the matrix, and  $R, T$  have the usual meaning. The results of the present study, as depicted in Figs. 5(A) and (B), show the growth of  $\beta$ -Si<sub>3</sub>N<sub>4</sub> grains along the length and width directions. The slopes, corresponding to the growth exponents of the growth equation, are calculated to be close to 3 and 5 for length and width directions, respectively. Table II lists the differences in growth exponents along both directions. Figure 6 gives the resulting variations of the aspect ratio with sintering time.

Based on our experimental results, the growth behavior of  $\beta$ -Si<sub>3</sub>N<sub>4</sub> grains seems to agree with the following empirical equation:

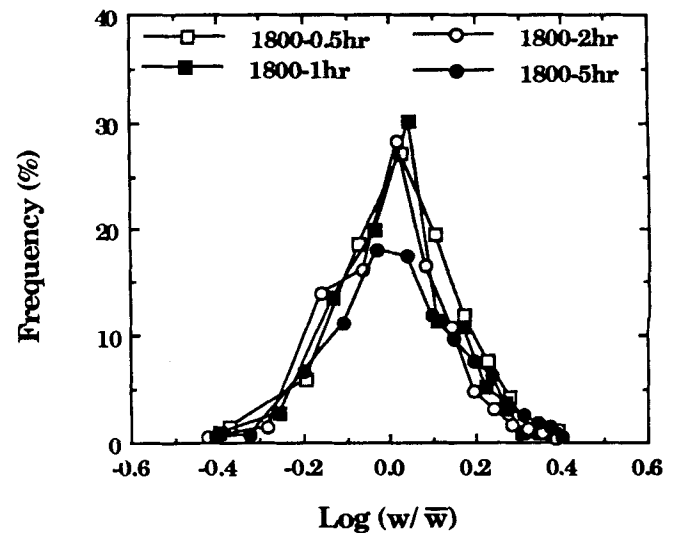
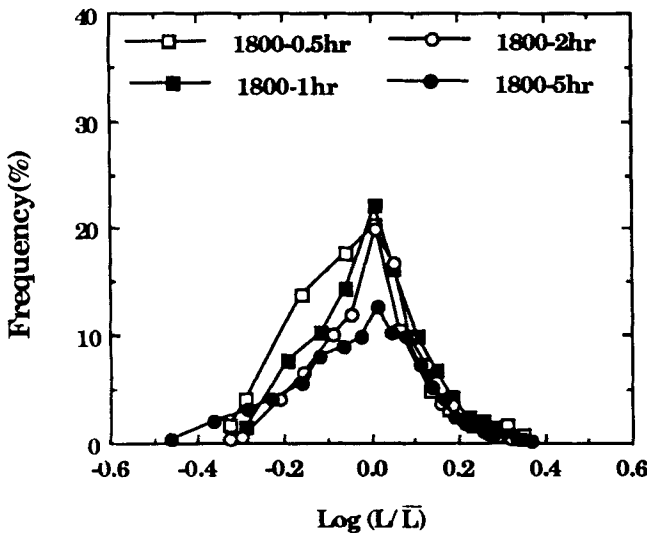


Fig. 4. Normalized grain size distributions of B10Y-Si<sub>3</sub>N<sub>4</sub> isothermally sintered at 1800°C. Distributions become broader as sintering time increases.

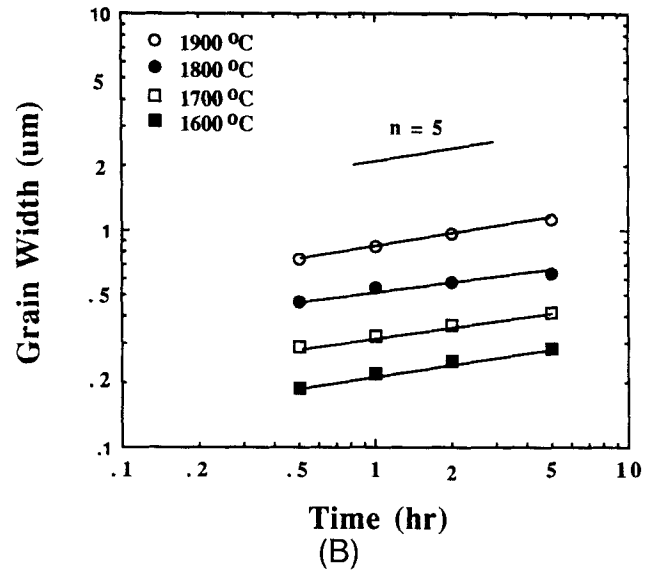
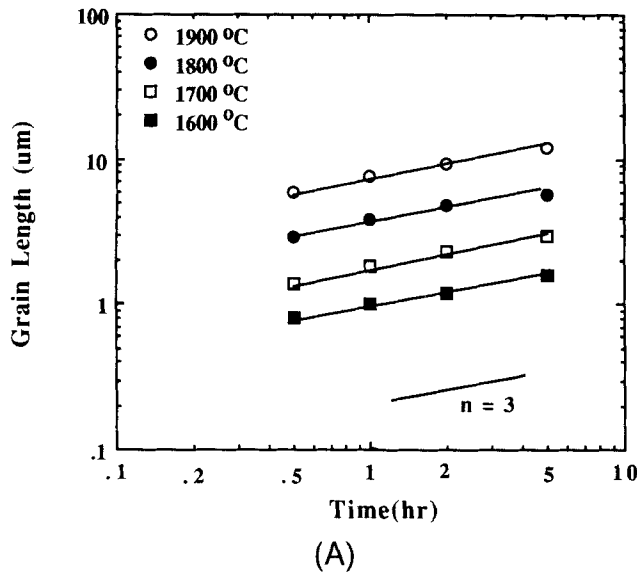


Fig. 5. (A) Grain growth behavior of B10Y-Si<sub>3</sub>N<sub>4</sub> in length direction. Samples were sintered under 10-atm N<sub>2</sub>. (B) Grain growth behavior of B10Y-Si<sub>3</sub>N<sub>4</sub> in width direction. Samples were sintered under 10-atm N<sub>2</sub>.

$$L^3 = K_L t \quad \text{or} \quad L = (K_L t)^{1/3} \quad (5)$$

$$W^5 = K_W t \quad \text{or} \quad W = (K_W t)^{1/5} \quad (6)$$

The rate constant  $K$  can be expressed in terms of the Arrhenius equation separately:

$$K_L = K_{0L} \exp\left(-\frac{Q_L}{RT}\right) \quad (7)$$

Table II. Measured Rate Constants and Exponents of  $\beta$ -Si<sub>3</sub>N<sub>4</sub> Ceramics Sintered under 10-atm N<sub>2</sub>

T(°C)	$n_1$	$K_L^*$ ( $\mu\text{m}^3/\text{h}$ )	$n_2$	$K_W^{\dagger}$ ( $\mu\text{m}^5/\text{h}$ )	$\Delta n^{\ddagger}$
1900	3.12	438.976	5.46	0.4385	0.138
1800	2.86	58.864	5.45	0.0459	0.166
1700	2.80	6.383	5.31	0.0036	0.169
1600	3.07	1.049	5.21	0.0005	0.134

$$*K_{0L} = 1.226 \times 10^{10} \mu\text{m}^3/\text{h}, \quad \dagger K_{0W} = 1.328 \times 10^{18} \mu\text{m}^5/\text{h}, \quad \ddagger \Delta n = \frac{1}{n_1} - \frac{1}{n_2}$$

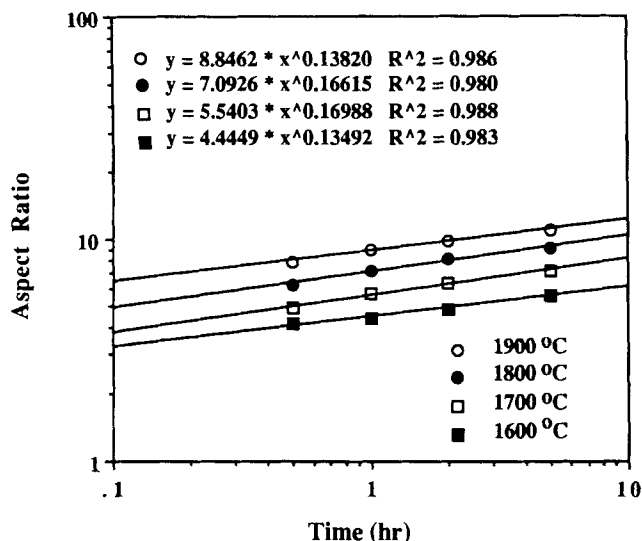


Fig. 6. Aspect ratios of B10Y-Si<sub>3</sub>N<sub>4</sub> as a function of sintering time at various isothermals. Function of the lines after curve fitting is indicated in the plot. Note that the slopes are approximately equal to  $\Delta n$ ,  $2/15$ , as derived in Eq. (9).

$$K_W = K_{0W} \exp\left(-\frac{Q_W}{RT}\right) \quad (8)$$

where  $Q_L$  and  $Q_W$  are activation energies, and  $K_{0L}$  and  $K_{0W}$  are preexponent factors in length and width directions, respectively. Figure 7 is a plot of rate constants versus reciprocal temperatures in log scale. Activation energies are calculated from the slope of the lines which correspond to 686 and 772 kJ/mol for length and width directions, respectively. It appears that the lower activation energy of grain growth in the length direction is equivalent to the growth preference, which was discussed earlier.

Since the growth exponents are experimentally determined as  $n_1 = 3$  and  $n_2 = 5$ , then the aspect ratio of  $\beta$ -Si<sub>3</sub>N<sub>4</sub> can be written as

$$\begin{aligned} \text{AR} &= \frac{L}{W} = \frac{(K_L)^{1/3}}{(K_W)^{1/5}} t^{(1/3)-(1/5)} \\ &= \left(\frac{K_L^{1/3}}{K_W^{1/5}}\right) t^{2/15} \end{aligned} \quad (9)$$

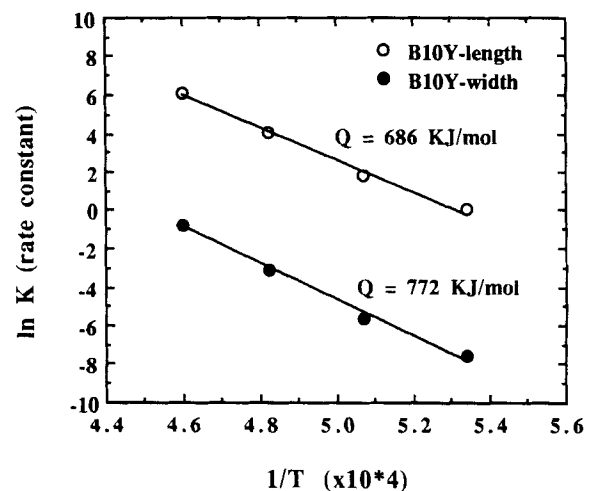


Fig. 7. Rate constants of grain growth of B10Y-Si<sub>3</sub>N<sub>4</sub> along length and width directions are plotted with respect to reciprocal temperature. Activation energies are calculated from the slope of the lines.

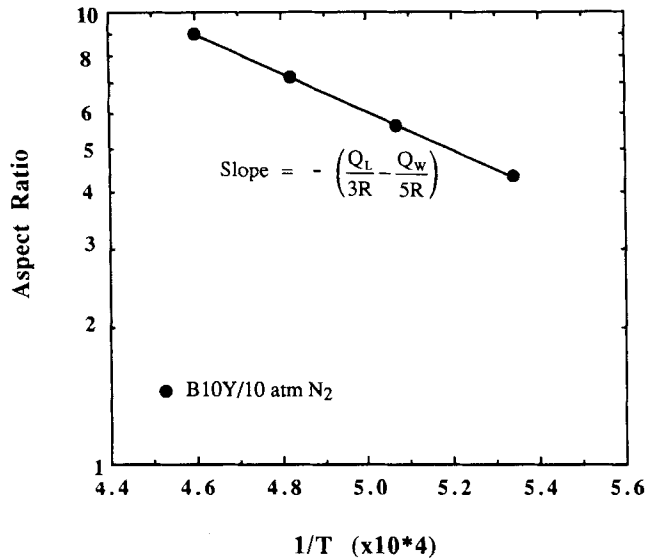


Fig. 8. The aspect ratio is plotted with respect to reciprocal temperature. The slope related to activation energies is given in Eq. (11).

$$= \left( \frac{K_{0L}^{1/3}}{K_{0W}^{1/5}} \right) t^{2/15} \exp \left[ - \frac{\left( \frac{Q_L}{3} - \frac{Q_W}{5} \right)}{RT} \right] \quad (10)$$

Therefore,

$$\ln AR = \ln \left( \frac{K_{0L}^{1/3}}{K_{0W}^{1/5}} \right) + \frac{2}{15} \ln t - \frac{\left( \frac{Q_L}{3} - \frac{Q_W}{5} \right)}{RT} \quad (11)$$

A slope of 2/15 can be obtained when a plot of ln (AR) vs ln (t) is made. Also, a slope of minus [(Q<sub>L</sub>/3) - (Q<sub>w</sub>/5)]/R can be obtained from the plot of ln (AR) vs 1/T. Figure 6 shows the trend of the aspect ratio with respect to the sintering time. All these slopes are approximately equal to 2/15. The slope of 2/15 is equivalent to the difference of reciprocal growth exponents in both directions, (1/3) - (1/5) = 2/15, which were obtained previously. Figure 8 illustrates the dependence of the aspect

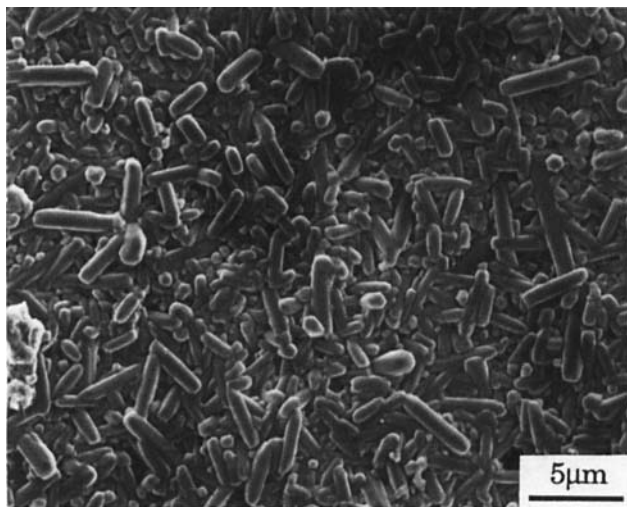
ratio with respect to the sintering temperature. The slope proves to be equal to the value of -(Q<sub>L</sub>/3 - Q<sub>w</sub>/5)/R, which was derived from Eq. (11). It appears, therefore, that the grain growth mechanisms along the length and width directions are revealed for the grain growth of  $\beta$ -Si<sub>3</sub>N<sub>4</sub> under N<sub>2</sub> pressure.

Hwang<sup>4</sup> and Mitomo<sup>11</sup> have studied the grain growth of Si<sub>3</sub>N<sub>4</sub> and independently obtained the growth exponents of n<sub>1</sub> = n<sub>2</sub> = 3. Thus, the aspect ratio of Si<sub>3</sub>N<sub>4</sub> grains in Eq. (3) can be further reduced to

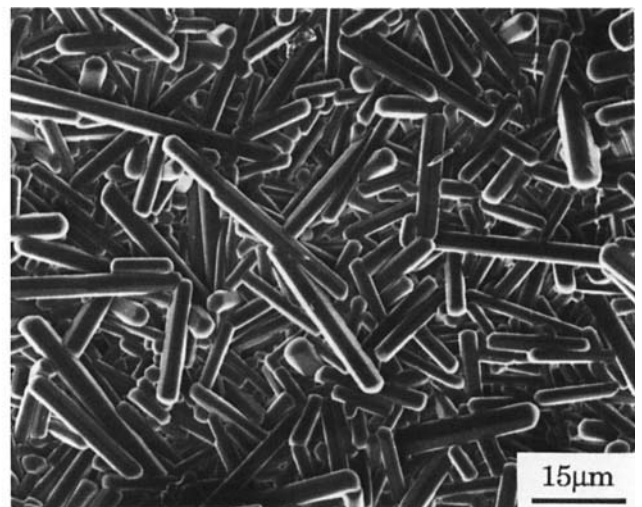
$$AR = \left( \frac{K_L}{K_W} \right)^{1/3} \quad (12)$$

For the same system at a specific temperature, the rate constants, K<sub>L</sub> and K<sub>w</sub>, in Eqs. (1) and (2) should remain unchanged, because rate constant varies only with temperature. This implies that the aspect ratio expressed in Eq. (12) should equal a constant during isothermal sintering. However, this conclusion conflicts with our observation in this study. The micrographs in Fig. 9 show specimens that were isothermally sintered at 1900°C for various lengths of time. The specimens were overetched and the micrographs were taken correspondingly as 3-dimensional microstructures in which elongated  $\beta$ -Si<sub>3</sub>N<sub>4</sub> grains can be observed directly. The aspect ratios of the samples appear to increase with increasing sintering time during isothermal sintering under high nitrogen pressure, indicating that Eq. (12) is not valid, since aspect ratio is still a function of sintering time. There is a further indication that the rate exponents of these two directions differ with each other.

The activation energy of 686 kJ/mol along the length direction lies in the range of 580–730 kJ/mol,<sup>23–25</sup> which is equivalent to the activation energy of Si diffusion in silicate glasses. Consequently, the grain growth mechanism of  $\beta$ -Si<sub>3</sub>N<sub>4</sub> along the length direction would be diffusion-controlled. The growth rate in the width direction was much slower than in the length direction. This can be interpreted by using Jackson's model<sup>16</sup> of the roughness of the solid/liquid interface ( $\alpha$ ). According to this model, Hwang<sup>4</sup> calculated the  $\alpha$ 's to be 2.05 and 1.75 at 1800°C for the (100) prism and (001) basal planes of  $\beta$ -Si<sub>3</sub>N<sub>4</sub>, respectively. An  $\alpha > 2$  represents a relatively smooth plane in the solid/liquid interface. This smoothness was also verified through transmission electron microscopy performed by Hwang.<sup>4</sup> It is this smoothness that results in the low precipitation rate of  $\beta$ -Si<sub>3</sub>N<sub>4</sub> on the prism plane, which might increase the kinetic barrier for grain growth of  $\beta$ -Si<sub>3</sub>N<sub>4</sub> along the width direction. The high activation energy (772 kJ/mol) for grain



(A)



(B)

Fig. 9. Micrographs of overetched B10Y-Si<sub>3</sub>N<sub>4</sub> ceramics show an increasing aspect ratio during isothermal sintering at 1900°C for (A) 0.2 h, (B) 24 h.

growth along the width direction is also indicative of this phenomenon.

Grest, Srolovitz and Anderson<sup>17</sup> have developed a model of grain growth with a case of anisotropic grain boundary energies, using a Monte Carlo computer simulation technique. They found that the anisotropic grain boundary energies can result in preferred grain growth. The resulting growth exponent can increase from  $n = 2.4$  for an isotropic case up to  $n = 4$  for the extreme anisotropic case. It appears that the anisotropic grain boundary energies might be a driving force that results in the change of the growth exponent from 3 to 5 for the width direction of  $\beta$ -Si<sub>3</sub>N<sub>4</sub>.

#### IV. Conclusion

Grain growth of  $\beta$ -Si<sub>3</sub>N<sub>4</sub> sintered in 10-atm N<sub>2</sub> pressure at 1600° to 1900°C follows the empirical grain growth equation with the growth exponents of 3 and 5 for length and width directions, respectively. This dissimilarity of growth exponents is most likely due to the anisotropic grain boundary energies. The aspect ratio is found to be proportional to 2/15 power of sintering time. The activation energy is 686 kJ/mol for grain growth along the length direction, which is equivalent to the energy for Si diffusion in silicate glasses. The high activation energy of 772 kJ/mol for growth along the width direction is probably due to the relative smoothness of the (100) prism plane.

#### References

- <sup>1</sup>J. Yamaguchi, "Isuzu's State-of-the-Art Ceramic Diesel Engine," *Automot. Eng.*, **96** [3] 78–79 (1988).
- <sup>2</sup>D. W. Richerson, "Evolution in The U.S. of Ceramic Technology for Turbine Engines," *Am. Ceram. Soc. Bull.*, **64** [2] 282–86 (1985).
- <sup>3</sup>E. Tani, S. Umabayashi, K. Kishi, K. Kobayashi, and M. Nishijima, "Gas-Pressure Sintering of Si<sub>3</sub>N<sub>4</sub> with Concurrent Addition of Al<sub>2</sub>O<sub>3</sub> and 5 wt% Rare Earth Oxide: High Fracture Toughness Si<sub>3</sub>N<sub>4</sub> with Fiber-like Structure," *Am. Ceram. Soc. Bull.*, **65** [9] 1311–15 (1986).
- <sup>4</sup>C. M. Hwang, "The System of Sialon–Y<sub>3</sub>Al<sub>5</sub>O<sub>12</sub> and Sialon–Cordierite: Sintering and Grain Growth"; Ph.D. Thesis. The University of Michigan, Ann Arbor, MI, 1988.
- <sup>5</sup>G. Ziegler, J. Heinrich, and G. Wotting, "Review: Relationships between Processing, Microstructural and Properties of Dense and Reaction-Bonded Silicon Nitride," *J. Mater. Sci.*, **22**, 3041–86 (1987).
- <sup>6</sup>L. J. Bowen, R. J. Weston, T. G. Carruthers, and R. J. Brook, "Hot-Pressing and the  $\alpha$ - $\beta$  Phase Transformation in Silicon Nitride," *J. Mater. Sci.*, **13**, 341–50 (1978).

<sup>7</sup>J. Heinrich, E. Backer, and M. Bohmer, "Hot Isostatic Pressing of Si<sub>3</sub>N<sub>4</sub> Powder Compacts and Reaction-Bonded Si<sub>3</sub>N<sub>4</sub>," *J. Am. Ceram. Soc.*, **71** [1] C-28–C-31 (1988).

<sup>8</sup>N. Hirotsaki, A. Akada, and K. Matoba, "Sintering of Si<sub>3</sub>N<sub>4</sub> with the Addition of Rare-Earth Oxides," *J. Am. Ceram. Soc.*, **71** [3] C-144–C-147 (1988).

<sup>9</sup>M. Mitomo, "Pressure Sintering of Si<sub>3</sub>N<sub>4</sub>," *J. Mater. Sci.*, **11**, 1103–107 (1976).

<sup>10</sup>H. F. Priest, G. L. Priest, and G. E. Gazza, "Sintering of Si<sub>3</sub>N<sub>4</sub> under High Nitrogen Pressure," *J. Am. Ceram. Soc.*, **60** [1–2] 81 (1977).

<sup>11</sup>M. Mitomo, M. Tsutsumi, H. Tanaka, S. Uenosono, and F. Saito, "Grain Growth during Gas-Pressure Sintering of  $\beta$ -Silicon Nitride," *J. Am. Ceram. Soc.*, **73** [8] 2441–45 (1990).

<sup>12</sup>D. D. Lee, S. L. Kang, and D. N. Yoon, "Mechanism of Grain Growth and  $\alpha$ - $\beta'$  Transformation during Liquid-Phase Sintering of  $\beta'$ -Sialon," *J. Am. Ceram. Soc.*, **71** [9] 803–806 (1988).

<sup>13</sup>G. Wotting, B. Kanka, and G. Ziegler, "Microstructural Development, Microstructural Properties of Dense Silicon Nitride"; pp. 83–96 in *Non-oxide Technical and Engineering Ceramics*. Edited by S. Hampshire. Elsevier Applied Science, London, England, 1986.

<sup>14</sup>D. R. Messier, F. L. Riley, and R. J. Brook, "The  $\alpha/\beta$  Silicon Nitride Phase Transformation," *J. Mater. Sci.*, **13**, 1119–205 (1978).

<sup>15</sup>J. W. Cahn, "On the Morphological Stability of Growing Crystals"; pp. 681–90 in *Crystal Growth*. Edited by H. S. Peiser. Pergamon Press, Oxford, U.K., 1967.

<sup>16</sup>K. A. Jackson, "Mechanism of Growth"; pp. 174–86 in *Liquid Metals and Solidification*. American Society for Metals, Metals Park, OH, 1958.

<sup>17</sup>G. S. Grest, D. J. Srolovitz, and M. P. Anderson, "Computer Simulation of Grain Growth IV. Anisotropic Grain Boundary Energies," *Acta Metall.*, **33** [3] 509–20 (1985).

<sup>18</sup>F. S. Ham, "Theory of Diffusion-Limited Precipitation," *J. Phys. Chem. Solids*, **16**, 335 (1958).

<sup>19</sup>C. M. Hwang, T. Y. Tien, and I-W. Chen, "Anisotropic Grain Growth during Final Stage Sintering of Silicon Nitride Ceramics"; pp. 1034–39 in *Sintering '87*. Edited by S. Somiya, M. Shimada, M. Yoshimura, and R. Watanabe. Elsevier, Essex, England, 1988.

<sup>20</sup>S. Takajo, N. A. Kaysser, and G. Petzow, "Analysis of Particle Growth by Coalescence during Liquid Phase Sintering," *Acta Metall.*, **32** [1] 107–13 (1984).

<sup>21</sup>I. M. Lifshitz and V. V. Slyozov, "The Kinetics of Precipitation from Super-saturated Solid Solutions," *J. Phys. Chem. Solids*, **19** [1–2] 35–50 (1961).

<sup>22</sup>J. W. Martin; p. 25 in *Micromechanism in Particle-Hardened Alloys*. Cambridge University Press, Cambridge, U.K., 1980.

<sup>23</sup>H. A. Schaeffer, "Silicon and Oxygen Diffusion in Oxide Glasses"; pp. 311–25 in *Mass Transport Phenomena in Ceramics*. Edited by A. R. Cooper and A. H. Heuer. Plenum Press, New York, 1975.

<sup>24</sup>G. Brebec, R. Sella, J. Bevenot, and J. C. Martin, "Diffusion of Silicon in Vitreous Silica," *Acta Metall.*, **28** [3] 327–33 (1980).

<sup>25</sup>A. Bouarroudj, P. Goursat, and J. L. Bessen, "Oxidation Resistance and Creep Behavior of a Silicon Nitride Ceramic Densified with Y<sub>2</sub>O<sub>3</sub>," *J. Mater. Sci.*, **20** [4] 1150–59 (1985). □